ELSEVIER

Earth and Planetary Science Letters 160 (1998) 107–113

EPSL

Elastic properties of hydrous ringwoodite (γ-phase) in Mg_2SiO_4

Toru Inoue *, Donald J. Weidner, Paul A. Northrup, John B. Parise

Center for High Pressure Research and Department of Earth and Space Sciences, State University of New York at Stony Brook, Stony Brook, NY 11794-2100, USA

Received 12 August 1997; accepted 24 April 1998

Abstract

Single-crystal elastic properties of hydrous ringwoodite are reported for samples that were synthesized at 19 GPa and 1300ºC. The Mg/Si ratio is determined to be ~1.95 by EPMA, which is slightly lower than that of ideal anhydrous ringwoodite. The H_2O content determined by SIMS is ~2.2 wt%, resulting in the stoichiometry $Mg_{1.89}Si_{0.97}O_4H_{0.33}$. The lattice parameter ($a = 8.0786 \pm 4$ Å) and elastic constants were determined from a single crystal with X-ray diffractometry and Brillouin scattering spectroscopy. The crystal structure is cubic Fd3m, with a unit cell volume which is 0.51% larger than that of the anhydrous ringwoodite. The adiabatic single-crystal elastic moduli of hydrous ringwoodite, in GPa, are: $C_{11} = 281 \pm 6$, $C_{44} = 117 \pm 4$, $C_{12} = 92 \pm 5$. The isotropic properties of hydrous ringwoodite are $K_{VRH} = 155 \pm 4$ and $G_{VRH} = 107 \pm 3$ which are about 16 and 10% smaller than those of anhydrous ringwoodite. Thus hydrous ringwoodite, if present, drastically reduces the seismic velocity in the mantle transition zone relative to anhydrous ringwoodite. In addition, our results show that the anisotropy is enhanced relative to anhydrous ringwoodite. Using the present results, we discuss the 520 km seismic discontinuity in a wet mantle transition zone.

Keywords: elastic properties; olivine group; lattice parameters; single-crystals method

1. Introduction

Ringwoodite is considered to be the most abundant mineral between 520 km and 670 km depth in the transition zone of the mantle. Recently, Kohlstedt et al. [1] reported that the ringwoodite can include significant amounts (~several wt%) of H_2O in the crystal structure which may critically influence the elastic properties. Wadsleyite can also include significant amounts of H_2O (~3 wt%) in its crystal structure [2–4]. Yusa and Inoue [5] determined the compressibility of hydrous wadsleyite. The isothermal bulk modulus is 155 GPa, a value 5–11% smaller than that of anhydrous wadsleyite. Thus it is expected that H_2O will reduce the seismic velocity of both ringwoodite and wadsleyite but not of olivine, since olivine does not incorporate significant amounts of H_2O into its crystal structure. Thus, conclusions regarding mantle composition that are based on the difference between sound velocities of olivine and its high pressure forms [5–8] must be reconsidered as water is included in the system. Further, some seismological studies have suggested the existence of a 520 km seismic discontinuity and the wadsleyite to ringwoodite transformation is a

* Corresponding author. Present address: Department of Earth Sciences, Ehime University, Matsuyama 790-8577, Japan. Tel.: +81 (89) 927-9658; Fax: +81 (89) 927-9640; E-mail: inoue@sci.ehime-u.ac.jp

0012-821X/98/$19.00
PII S0012-821X(98)00077-6

candidate for this discontinuity (e.g. [9]). The effect of water on this boundary must also be examined.

To address these issues, we synthesized single crystals of the hydrous ringwoodite to determine the crystal structure and elastic properties of this phase. We report here the lattice parameter by single-crystal X-ray diffraction and the single-crystal elastic moduli of hydrous ringwoodite determined by Brillouin scattering spectroscopy for the first time.

2. Experimental

Single crystals of hydrous ringwoodite were synthesized at 19 GPa and 1300°C using an MA-8 type apparatus at SUNY Stony Brook (USSA-2000). Starting materials were a mixture of MgO–$Mg(OH)_2$–SiO_2 of 1 : 1 : 1 in molar ratio (Mg_2SiO_4–H_2O 11.3 wt%). This powder was enclosed in a platinum capsule. The run duration was approximately 60 min and to enhance the crystal growth, the *P*–*T* conditions appropriate for partial melting in the system Mg_2SiO_4–H_2O, i.e. just above the wet solidus, were selected.

The run products contained large crystals of hydrous ringwoodite (~100 μm), a dendritic texture (liquid) and small amounts of stishovite. The Mg/Si of the hydrous ringwoodite is approximately 1.95 ± 0.02 and the microprobe analysis weight total is 97.3 ± 1.4 wt% from the average of 8-point measurements by EPMA (Cameca) at SUNY Stony Brook. In addition, we measured the H_2O content (2.2 ± 0.2 wt%) by SIMS (Cameca IMS-3F: Tokyo Institute of Technology). These results are quite consistent and suggest a chemical formula of the present hydrous ringwoodite of $Mg_{1.89}Si_{0.97}O_4H_{0.33}$.

We selected a large and optically clear and untwinned single crystal for single-crystal X-ray and Brillouin scattering measurements. The size of the single crystal was $140 \times 130 \times 90$ μm. The crystal had several large growth faces.

The Brillouin spectroscopy method and the experimental setup used in the present study have been previously described in detail [10–12]. An argon ion laser operating at a wavelength of 5145 Å was used for the source. A 90° scattering geometry between the incident beam and the photon detection equipment was employed. The scattered signal was analyzed by a Fabry-Perot interferometer operating in triple-pass configuration. To minimize refraction effects at the surface of the crystal, all velocity measurements were made with the crystal immersed in refractive index liquid ($n_{5145\,Å} = 1.633$).

The crystal was oriented and the lattice parameter was determined on a four-circle X-ray diffractometer at SUNY Stony Brook. Upon transferring to the Brillouin spectrometer, the orientation is preserved to within about 0.5°.

3. Results and discussions

The present hydrous ringwoodite has a cubic structure (Fd3m), the same as the anhydrous ringwoodite. The lattice parameter, 8.0786 ± 4 Å, is 0.17% larger than that of anhydrous ringwoodite [13]. Consequently, the unit cell volume is 0.51% larger than that of anhydrous ringwoodite. The volume and stoichiometry taken together yield a density of 3.469 g/cm^3, which is 2.7% smaller than that of anhydrous ringwoodite (Table 1). Further details of the single-crystal X-ray study will be published elsewhere.

The refractive index was determined by immersion techniques to be 1.704 ± 2, which is slightly smaller than that of anhydrous ringwoodite (1.708 ± 2). Hydrous ringwoodite, being cubic, requires three elastic moduli to completely describe its single-crystal elastic character. A total of 19 independent acoustic velocities were determined from over 30 recorded Brillouin spectra. These velocities correspond to a variety of crystallographic directions and modes and represent a factor of 6 overestimation. The data were reduced using the method described by Weidner and Carleton [10]. They are $C_{11} = 281 \pm 6$, $C_{44} = 117 \pm 4$, and $C_{12} = 92 \pm 5$ (GPa), which are 14%, 7% and 18% smaller than

Table 1
Lattice parameters of ringwoodite (γ) and hydrous ringwoodite (hy-γ)

	a (Å)	*V* (Å^3)	ρ (g/cm^3)	
hy-γ	8.0786 ± 4	527.24	3.469	this study
γ	8.0649 ± 1	524.56	3.563	Sasaki et al. [13]

Table 2
Single-crystal elastic moduli of ringwoodite and hydrous ringwoodite

ij	C_{ij}, GPa	S_{ij}, GPa^{-1}
Hydrous ringwoodite		
11	281 ± 6	0.00424
44	117 ± 4	0.00857
12	92 ± 5	−0.00104
Ringwoodite		
11	327 ± 4	0.00370
44	126 ± 2	0.00792
12	112 ± 3	−0.00094

The data of ringwoodite are from Weidner et al. [12].

those of anhydrous ringwoodite [12], respectively (Table 2). Information concerning the acoustic velocities is given in Table 3, including a comparison of the observed and model velocities. The model deviates from the observations by 0.12 km/s (rms).

Fig. 1 illustrates the observed and model velocities as a function of crystallographic orientation. In this figure, the data are projected onto the nearest a–b plane, preserving the difference between the measured and observed values. Each of the a–b planes are equivalent and symmetric by the cubic nature of the crystal.

Fig. 2 compares the acoustic velocities of the present hydrous ringwoodite and anhydrous ringwoodite as a function of crystallographic orientation. In the direction parallel to the principal axis [1,0,0], the compressional velocity and shear velocity of hydrous ringwoodite are 6.0% and 2.3% smaller than those of anhydrous ringwoodite, respectively. Whereas in [1,1,0] direction, the values are both 5.0% smaller than those of anhydrous ringwoodite. Thus the anisotropy between V_{sh} and V_{sv} is enhanced in the case of hydrous ringwoodite. The degrees of the anisotropy $(V_{sh}/V_{sv})^2$ are 0.808 for hydrous ringwoodite and 0.853 for anhydrous ringwoodite in

Table 3
Measured acoustic velocities as a function of propagation direction and polarization direction in hydrous ringwoodite

Propagation direction			Polarization direction			Observed velocity (km/s)	Model velocity (km/s)	Difference
n_1	n_2	n_3	u_1	u_2	u_3			
0.45	0.83	0.34	0.48	0.80	0.37	9.14	9.34	−0.20
			−0.50	−0.10	0.86	5.73	5.64	0.09
0.90	0.20	0.39	0.87	0.23	0.44	9.41	9.24	0.17
			−0.09	0.95	−0.31	5.99	5.74	0.25
0.71	0.59	0.39	0.69	0.59	0.41	9.27	9.42	−0.15
			−0.22	−0.37	0.90	5.64	5.58	0.06
−0.26	0.96	0.11	−0.31	0.94	0.12	9.35	9.12	0.23
			0.25	−0.05	0.97	5.78	5.78	0.00
0.07	0.97	0.23	0.98	−0.04	−0.18	5.83	5.79	0.04
0.15	0.96	0.25	0.18	0.94	0.30	9.19	9.13	0.06
			0.92	−0.05	−0.39	5.71	5.76	−0.05
0.81	−0.54	0.23	−0.14	0.24	0.96	5.60	5.72	−0.12
−0.56	−0.10	−0.83	0.58	0.11	0.80	9.27	9.32	−0.05
			0.81	0.04	−0.59	5.08	5.31	−0.23
−0.17	−0.61	−0.78	0.19	0.62	0.76	9.36	9.35	0.01
			0.05	0.77	−0.64	5.28	5.27	0.01
−0.34	−0.47	−0.81	0.37	0.50	0.78	9.34	9.36	−0.02
			0.31	0.73	−0.61	5.37	5.39	−0.02
−0.47	−0.30	−0.83	0.50	0.32	0.80	9.27	9.34	−0.07

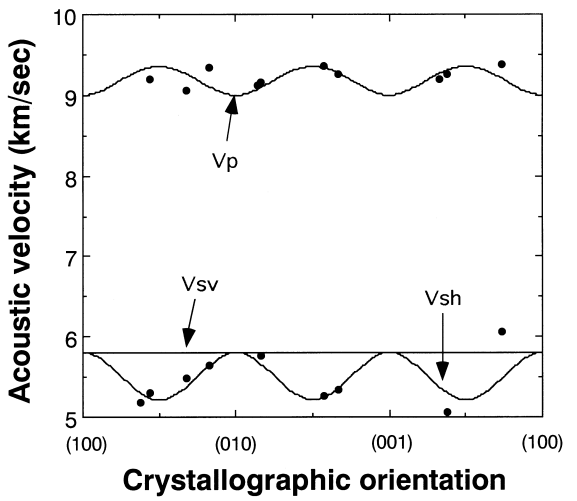

Fig. 1. Observed (dots) and calculated (solid line) acoustic velocities of single-crystal hydrous ringwoodite as a function of crystallographic orientation. The observed values are projected onto the nearest principal plane, preserving the difference between the observed and calculated velocity.

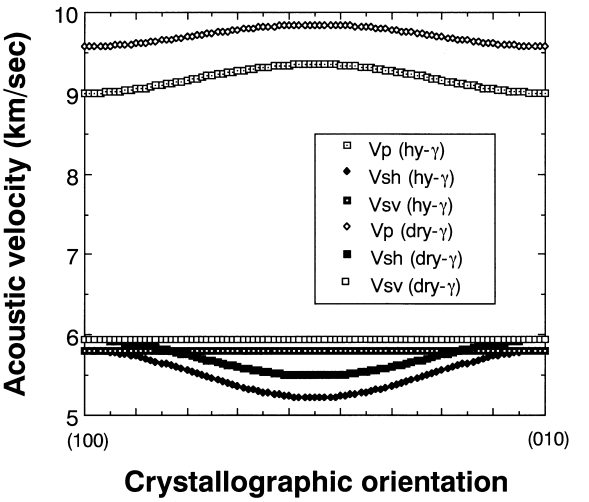

Fig. 2. Comparison with the acoustic velocities between anhydrous ringwoodite (dry-γ) and hydrous ringwoodite (hy-γ) as a function of crystallographic orientation.

the direction [1,1,0]. Table 4 compares the aggregate elastic properties of hydrous ringwoodite and anhydrous ringwoodite. The bulk and shear moduli are 155 ± 4 and 107 ± 3 (GPa), respectively, which are 16% and 10% smaller than those of anhydrous ringwoodite. The compressional and shear velocities are 9.27 km/s and 5.56 km/s, which are 5.3% and 3.6% smaller than those of anhydrous ringwoodite. Thus hydrous ringwoodite would drastically reduce the seismic velocity in the mantle transition zone relative to anhydrous ringwoodite.

Yusa and Inoue [5] reported the compressibility of hydrous wadsleyite and showed that the bulk modulus was 5–11% smaller than that of anhydrous wadsleyite, demonstrating similar behavior to hydrous ringwoodite, but with a much larger reduction for hydrous ringwoodite than that of hydrous wadsleyite, in spite of lower H_2O content of hydrous ringwoodite relative to hydrous wadsleyite ($\sim$2.7 wt% of H_2O).

We calculated the density and bulk sound velocity for olivine, wadsleyite, ringwoodite, hydrous wadsleyite and hydrous ringwoodite of the pure magnesium system as a function of pressure using the Birch–Murnaghun equation of state (Fig. 3). Olivine does not include a significant amount of H_2O in the crystal structure, so the properties for olivine reflect those of the anhydrous state. Since the thermal properties of hydrous wadsleyite and hydrous ringwoodite have not yet been measured, the above parameters were calculated at room temperature. Further since the pressure dependences of the bulk modulus of hydrous wadsleyite and hydrous ringwoodite are unknown, they were assumed to be the same as those for the dry form. We further assume that the effect of iron on the density and sound velocities are the same for all polymorphs. So in the following discussion, we do not consider the effect of iron.

Table 4
Aggregate elastic properties of ringwoodite and hydrous ringwoodite

	V_p (km/s)	V_s (km/s)	K (GPa)	G (GPa)
Hydrous ringwoodite				
Reuss	9.26	5.55	155 ± 4	107 ± 3
Voigt	9.28	5.58	155 ± 4	108 ± 3
VRH	9.27	5.56	155 ± 4	107 ± 3
Ringwoodite				
Reuss	9.78	5.76	184 ± 2	118 ± 2
Voigt	9.80	5.78	184 ± 2	119 ± 2
VRH	9.79	5.77	184 ± 2	119 ± 2

The data of ringwoodite are from Weidner et al. [12]. VRH = Voigt–Reuss–Hill; V_p = longitudinal wave velocity; V_s = shear wave velocity; K = bulk modulus; G = shear modulus.

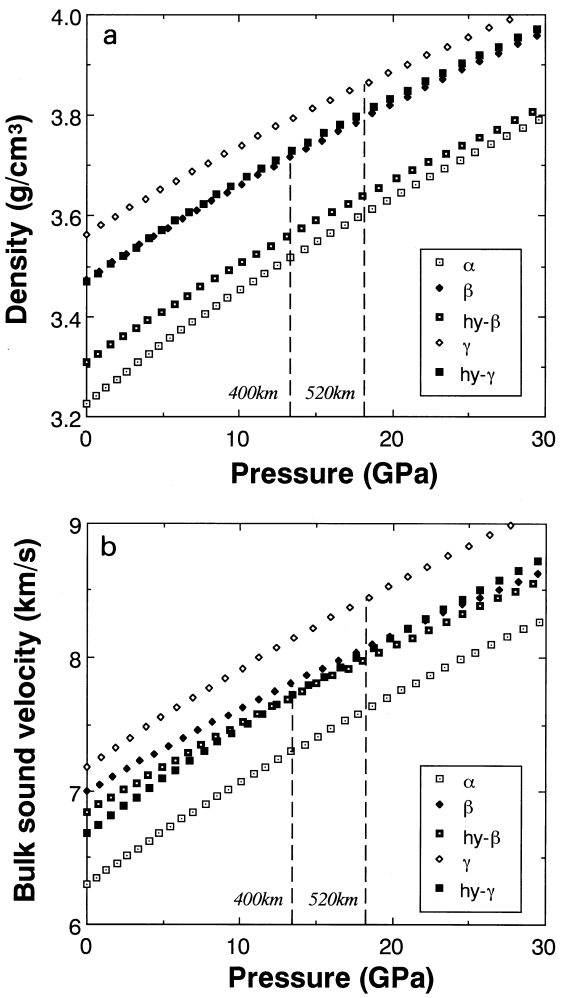

Fig. 3. The density (a) and bulk sound velocity (b) profiles of olivine (α), wadsleyite (β), ringwoodite (γ), hydrous wadsleyite (hy-β) and hydrous ringwoodite (hy-γ) as a function of pressure. The density and the bulk modulus data using the calculation are cited, as follows. Olivine: ρ, Ref. [18]; K_0, K_0', Ref. [19]. Wadsleyite: ρ, Ref. [20]; K_0, K_0', Ref. [19]. Ringwoodite: ρ, Ref. [13]; K_0, Ref. [12], K_0', Ref. [21]. Hydrous wadsleyite: ρ, Ref. [22]; K_0, Ref. [5], K_0', estimated the same as the dry form. Hydrous ringwoodite: ρ; K_0, this study, K_0', estimated the same as the dry form.

The density of hydrous ringwoodite is almost the same as that of anhydrous wadsleyite (Fig. 3a). But at higher pressure, the density of hydrous ringwoodite becomes larger than that of anhydrous wadsleyite because of the difference of the compressibilities. The densest form is anhydrous ringwoodite, and then hydrous ringwoodite, anhydrous wadsleyite, hydrous wadsleyite and olivine.

Table 5
Difference of the density and the bulk sound velocity at 400 km and 520 km depth in dry and wet mantle

	$\Delta\rho$ (g/cm^3)	ΔV_b (km/s)	Impedance difference (%)
~400 km depth (~13.5 GPa)			
$\alpha \rightarrow \beta$	0.20 (5.7%)	0.51 (7.0%)	13.0
$\alpha \rightarrow$ hy-β	0.05 (1.3%)	0.41 (5.6%)	7.0
~520 km depth (~17.5 GPa)			
$\beta \rightarrow \gamma$	0.07 (1.8%)	0.37 (4.5%)	6.4
hy-$\beta \rightarrow$ hy-γ	0.16 (4.5%)	0.05 (0.7%)	5.2

ρ = density; V_b = bulk sound velocity; impedance = $\rho \times V_b$.

The bulk sound velocities of hydrous wadsleyite and hydrous ringwoodite are much smaller than those of anhydrous wadsleyite and ringwoodite, respectively (Fig. 3b). So the velocity jump from olivine to wadsleyite and from wadsleyite to ringwoodite in a wet mantle becomes smaller than for the case of a dry mantle. It is noteworthy that the velocity reduction from anhydrous ringwoodite to hydrous ringwoodite is much larger than that from anhydrous wadsleyite to hydrous wadsleyite.

We estimated the impedance difference in the olivine–wadsleyite and the wadsleyite–ringwoodite transformations under dry and wet conditions (Table 5). At around 13.5 GPa (corresponding to 400 km depth), the difference between olivine and wadsleyite under wet conditions is 7.0%, whereas it is 13.0% for dry conditions. Thus the difference of the wet state is about half that of the dry state. Yusa and Inoue [5] use this information and conclude that a pyrolite composition with 1–2 wt% H_2O satisfies the magnitude of the observed 410 km seismic discontinuity.

At around 18 GPa (corresponding to 520 km depth), the impedance difference between wadsleyite and ringwoodite for both the dry and wet conditions are similar (5–6%). We might expect this impedance jump to be seismically observable if the wadsleyite–ringwoodite transformation depth is narrow. But under dry conditions, the boundary is relatively wide (~2 GPa, corresponding to 60 km wide) [14], and it may not be possible to detect a seismic velocity jump in a dry mantle. Recently, we examined the

wadsleyite–ringwoodite phase boundary under wet conditions, with the results that the transition region becomes narrower and deeper (less than 0.5 GPa, corresponding to less than 15 km) [15,16]. This implies that the 520 km discontinuity could be observed in a wet mantle transition zone. Shearer [9] reported the existence of 520 km seismic discontinuity, and the amplitudes of the apparent Pp520p and Ss520s phases are consistent with an impedance contrast at 520 km of ~3%, for a transition region less than about 25 km thick. These results are consistent with our present results. Lateral variations in the depth and strength of the 520 km discontinuity [17] may indicate lateral variations of mantle water.

The present study illustrates the behavior expected of a fully hydrated mantle transition zone. Dry wadsleyite and hydrous wadsleyite, and dry ringwoodite and hydrous ringwoodite become solid solutions, so we can estimate the effect of a partially saturated mantle transition zone by combining the results of the dry and wet systems.

Of course, the shear modulus of hydrous wadsleyite remains to be determined and is important in calculating the compressional and shear wave velocity jump at both the 400 km and the 520 km discontinuities in a wet mantle.

Acknowledgements

We thank H. Yurimoto for help on SIMS analysis and R.P. Rapp for instruction on EPMA analysis. We wish to thank R.C. Liebermann and T. Irifune for their useful comments. We acknowledge the constructive review of T.S. Duffy as well as the comments of two anonymous reviewers. This study was supported by a grant from the National Science Foundation (9506483) to JBP and DJW. ***[RO]***

References

[1] D.L. Kohlstedt, H. Keppler, D.C. Rubie, Solubility of water in the α, β and γ phases of $(Mg,Fe)_2SiO_4$, Contrib. Mineral. Petrol. 123 (1996) 345–357.

[2] T. Gasparik, The role of volatiles in the transition zone, J. Geophys. Res. 98 (1993) 4287–4299.

[3] T. Inoue, Effect of water on melting phase relations and melt composition in the system Mg_2SiO_4–$MgSiO_3$–H_2O up to 15 GPa, Phys. Earth Planet. Inter. 85 (1994) 237–263.

[4] T. Inoue, Y. Yurimoto, T. Kudoh, Hydrous modified spinel, $Mg_{1.75}SiH_{0.5}O_4$: a new water reservoir in the mantle transition region, Geophys. Res. Lett. 22 (1995) 117–120.

[5] H. Yusa, T. Inoue, Compressibility of hydrous wadsleyite (β-phase) in Mg_2SiO_4 by high pressure X-ray diffraction, Geophys. Res. Lett. 24 (1997) 1831–1834.

[6] T.S. Duffy, D.L. Anderson, Seismic velocities in mantle minerals and the mineralogy of the upper mantle, J. Geophys. Res. 94 (1989) 1895–1912.

[7] H. Sawamoto, D.J. Weidner, S. Sasaki, M. Kumazawa, Single-crystal properties of the modified spinel (beta) phase of magnesian orthosilicate, Science 224 (1984) 749–751.

[8] T.S. Duffy, C.-S. Zha, R.T. Downs, H.-K. Mao, R.J. Hemley, Elasticity of forsterite to 16 GPa and the composition of the upper mantle, Nature 378 (1995) 170–173.

[9] P.M. Shearer, Seismic imaging of upper-mantle structure with new evidence for a 520-km discontinuity, Nature 344 (1990) 121–126.

[10] D.J. Weidner, H.R. Carleton, Elasticity of coesite, J. Geophys. Res. 82 (1977) 1334–1346.

[11] D.J. Weidner, M.T. Vaughan, A technique for measuring single-crystal elastic properties of high pressure phases, in: D. Timmerhaus, M.S. Barber (Eds.), High Pressure Science and Technology, Vol. 2, 1979, pp. 85–90.

[12] D.J. Weidner, H. Sawamoto, S. Sasaki, M. Kumazawa, Elasticity of Mg_2SiO_4 spinel, J. Geophys. Res. 89 (1984) 7852–7860.

[13] S. Sasaki, C.T. Prewitt, S. Sato, E. Ito, Single crystal X-ray studies of γ-Mg_2SiO_4, J. Geophys. Res. 87 (1982) 7829–7832.

[14] M. Akaogi, E. Ito, A. Navrotsky, Olivine-modified spinel–spinel transitions in the system Mg_2SiO_4–Fe_2SiO_4: calorimetric measurements, thermochemical calculation, and geophysical application, J. Geophys. Res. 94 (1989) 15671–15685.

[15] T. Inoue, J. Chen, D.J. Weidner, H. Yurimoto, Phase boundaries between α, hydrous β and hydrous γ in the system Mg_2SiO_4–H_2O, Eos 77 (46) (1996) F682.

[16] T. Inoue, J. Chen, D.J. Weidner, H. Kagi, H. Yurimoto, P.A. Northrup, J.B. Parise, Phase boundaries between olivine(α), hydrous wadsleyite(β) and hydrous ringwoodite(γ) and their elastic properties, AIRAPT abstr., 1997, p. 489.

[17] J. Revenaugh, T.H. Jordan, Mantle layering from ScS reverberations, 3, The upper mantle, J. Geophys. Res. 96 (1991) 19781–19810.

[18] K. Fugino, S. Sasaki, Y. Takeuchi, R. Sadanaga, X-ray determination of electron distributions in forsterite, fayalite, and tephroite, Acta Crystallogr. B37 (1981) 513–518.

[19] B. Li, G.D. Gwanmesia, R.C. Liebermann, Sound velocities of olivine and beta polymorphs of Mg_2SiO_4 at Earth's transition zone pressures, Geophys. Res. Lett. 23 (1996) 2259–2262.

[20] H. Horiuchi, H. Sawamoto, β-Mg_2SiO_4: single-crystal X-ray diffraction study, Am. Mineral. 66 (1981) 568–575.

[21] S.M. Rigden, G.D. Gwanmesia, J.D. FitzGerald, I. Jackson,

R.C. Liebermann, Spinel elasticity and the seismic structure of the transition zone of the mantle, Science (1991).
[22] Y. Kudoh, T. Inoue, H. Arashi, Structure and crystal chemistry of hydrous wadsleyite, $Mg_{1.75}SiH_{0.5}O_4$: Possible hydrous magnesium silicate in the mantle transition zone, Phys. Chem. Miner. 23 (1996) 461–469.